2021-03

Experimental Investigation on Thermo-Hydraulic Performance of Triangular Cross-Corrugated Flow Passages

Krishnan, Easwaran N

Elsevier

Easwaran N. Krishnan, Hadi Ramin, A. Guruabalan, Carey J. Simonson, (2021). Experimental investigation on thermo-hydraulic performance of triangular cross-corrugated flow passages, International Communications in Heat and Mass Transfer, 122, 105160. https://doi.org/10.1016/j.icheatmasstransfer.202

https://hdl.handle.net/10388/14880

https://doi.org/10.1016/j.icheatmasstransfer.2021.105160

Experimental Investigation on Thermo-Hydraulic Performance of Triangular Cross-Corrugated Flow Passages

Easwaran N. Krishnan, Hadi Ramin, A. Guruabalan and Carey J. Simonson

Department of Mechanical Engineering, University of Saskatchewan 57 Campus Dr, Saskatoon, SK S7N 5A9

ABSTRACT

Heat exchangers made of corrugated flow passages generally have better thermo-hydraulic performance compared to parallel flow passages. The corrugation angle (β), corrugation pattern, and the ratio of depth to pitch (h_{ch}/P_{ch}) are critical geometrical parameters influencing the heat transfer and pressure drop in corrugated flow passages. This paper experimentally investigates heat transfer and pressure drop characteristics of triangular-shaped cross-corrugated flow passages for the range of $25°<\beta<75°$ and $0.13<h_{ch}/P_{ch}<0.36$. Experiments are performed using representative compact heat exchangers in a small-scale test facility. This study also reports the effects of plate geometry on heat transfer and pressure drop and provides correlations for the average Nusselt number and friction factor. A detailed comparison of test data with relevant literature is also presented. Results of this study will be useful to manufactures and designers for developing high-performance heat exchangers.

Keywords: Corrugated passages, Heat exchangers, Pressure drop, Friction factor, Nusselt number.

NOMENCLATURE

A_{ht}	Heat transfer area (m^2)	ΔP	Pressure drop (Pa)
C	Ratio of specific heats	Nu	Nusselt number
D_h	Hydraulic diameter (m)	Re	Reynolds number
f	Friction factor	T	Temperature (°C)
h	Average heat transfer coefficient ($W\ m^{-2}\ K^{-1}$)	t_p	Plate thickness (m)
h_{ch}	Channel height/ corrugation depth (m)	V_{ch}	Channel velocity ($m\ s^{-1}$)
k_f	Thermal conductivity of air ($W\ m^{-1}\ K^{-1}$)	**Greek letters**	
L	Plate length before corrugation (m)	β	Corrugation angle (°)
NTU_o	Overall number of transfer units	ε	Sensible effectiveness
n_f	Number of flow channels	**Abbreviations**	
P_{ch}	Corrugation pitch (m)	EX	Exchanger
Pr	Prandtl number	min	Minimum

1. INTRODUCTION

Plate heat exchangers and fixed-bed regenerators are commonly used in many applications such as power plants, food, and chemical industries because of their compactness, high performance, and ease of cleaning [1–4]. The geometry of metallic plates of these exchangers significantly influences its thermo-hydraulic performance. Studies have shown that cross corrugations in plates improve the heat transfer by 20-30% since it generates turbulence at low Reynolds numbers [5–8]. Manufacturers have specifically designed corrugation patterns and stacking arrangements to achieve a high heat transfer rate with minimum pumping power.

The critical design parameters which affect the heat transfer and pressure drop in cross corrugated plates are corrugation angle (β), corrugation pattern, and the ratio of depth to pitch (h_{ch}/P_{ch}) of the plates [1,9–12]. Several experimental and CFD investigations have reported the fundamental nature of the flow for sinusoidal cross-corrugated passages [7,10–16] and shown that the fluid never attains a fully developed condition because of the sudden changes in direction due to corrugations and continuous deterioration of the boundary layer [13,17]. In addition to mixing, the small hydraulic diameter and secondary flow formation (Görtler vortices) also contribute to the enhanced thermo-hydraulic performance of corrugated plates [18]. Focke et al. [11] and Zimmer et al. [19] categorized the flow patterns inside the cross corrugated flow channels into furrow flow or zig-zag flow, longitudinal or corkscrew flow, and mixing flow at low, intermediate, and high corrugation angles, respectively. Later, Kifah [13] showed that the Reynolds numbers or mass flow rates would also affect the transition of flow structures by CFD analysis.

Focke et al. [11] developed correlations for Coburn j factor and friction factor as a function of Reynolds number and suggested that the heat transfer is maximum at corrugation angles 72° to 80°. However, Gasier and Kottke [12] experimentally showed that optimum corrugation angles for maximum heat transfer would also depend on the ratio of corrugation depth to pitch. Later, Dovic and Svaic [10] validated the results of Gasier and Kottke [12] using flow visualization techniques. Sparrow and Hossfeld's investigation concludes that rounding of sharp edges of corrugations results in an 8-18% drop in Nusselt number [20] depending on the Reynolds number. Dovic and Svaic have proposed generalized correlations for friction factor and Nusselt number by modeling a single unit cell of the flow channel [21]. Their predictions have a maximum of 20-25% deviation from the experimental results. Muley and Manglik [9] also investigated the performance of plate heat exchangers having 30° and 60° corrugation angles and developed correlations for Nusselt

number and friction factor as functions of corrugation angle and area enlargement ratio. The heat transfer and pressure drop predictions from the reported correlations have significant discrepancies [7,11,19–21]. These could be due to insufficient test data and plate geometry information, test uncertainties, and complexities modeling the flow. Most studies on cross corrugated flow passages were focused on sinusoidal cross corrugated flow channels and their applications on plate heat exchangers. However, only a few works [22,23] were focused on heat transfer characteristics and pressure drop in triangular cross corrugated flow channels.

The objective of this paper is to study the thermo-hydraulic performance of triangular cross corrugated flow channels. Experiments are performed on seven representative compact exchangers. The effects of corrugation angle and ratio of corrugation depth on heat transfer and pressure drop are investigated. Correlations for the average Nusselt number and friction factor are also developed based on the test data. Finally, the test results are compared with similar results from the literature.

2. EXPERIMENTAL METHODOLOGY

2.1 Test facility

A small-scale test facility is used to measure the thermo-hydraulic performance of corrugated flow passages (or exchangers), as shown in Fig. 1 and 2. The exchanger is exposed to hot and cold airstreams alternatively with the help of a computer-controlled linear actuator unit. The duration for which the exchanger is exposed to hot and cold airstreams are called hot and cold periods, respectively. The exchanger stores heat from the airstream during the hot period and release the stored heat in the subsequent cold period. The inlets and outlets of the cold and hot airstreams are numbered as 1, 2, 3, and 4 in Fig. 1.

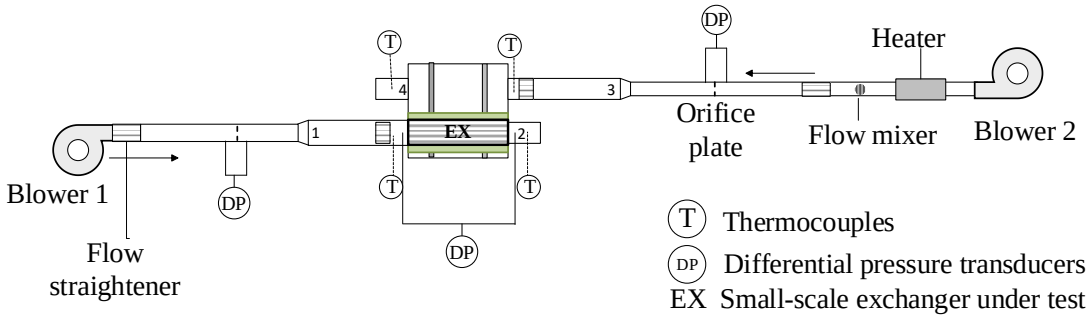

Fig. 1 Experimental facility to measure heat transfer and pressure drop in triangular cross-corrugated flow passages

The design and development of the test facility are reported in our previous publications in detail [24,25]. The flow rate, temperature, and pressure drop across the exchanger are measured using orifice plates, T-type thermocouples, and pressure transducers. The orifice plates are designed and installed according to the ISO standard 5167 guidelines [26]. The uncertainty in mass flow rates is evaluated from the uncertainty in pressure drop measurements across the orifice plates. The instrumentation details and their uncertainties are reported in Table 1. The overall heat balance was evaluated in all experiments, and the maximum difference between effectiveness changes was less than 5%. This difference could be due to the heat interaction between the test section and surroundings and the measurement uncertainties.

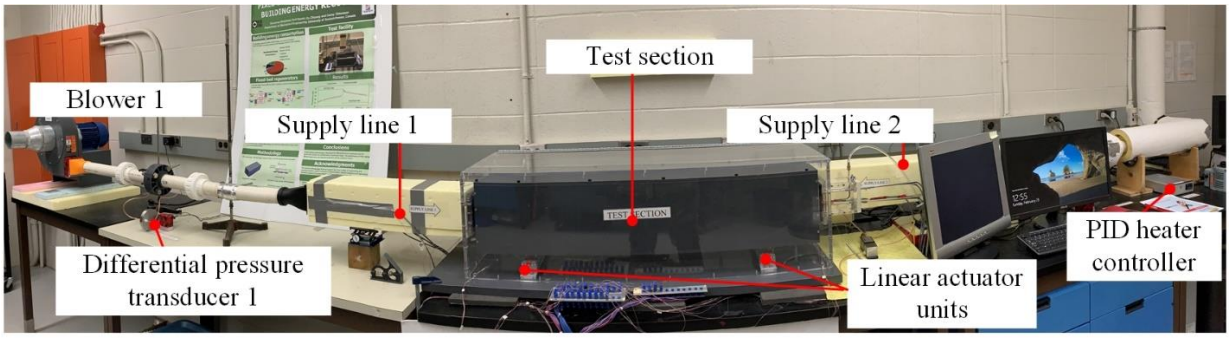

Fig. 2 Photograph of experimental facility

Table 1. Instruments specifications and calibration details.

Instrument	Measurement parameter	Manufacturer	Model	Calibration range	Total uncertainty
Thermocouples	Temperature	Omega	T- type	-20°C to 40°C	±0.2°C
Differential pressure transducer 1	Pressure drop across the exchanger	Validyne	DP 17	0-430 Pa	± 4 Pa
Differential pressure transducer 2	Pressure drop across the orifice plate	Validyne	DP 17	0-860 Pa	± 8 Pa

2.2 Exchanger geometry and performance parameters

The exchanger plates are made of corrugated aluminum sheets, and the arrangement of two consecutive plates is shown in Fig. 3. Both sides of the exchangers are covered with Styrofoam insulations, which act as sidewalls and reduce the exchanger's heat interaction with the surroundings. The corrugated plates are manufactured following industrial standards by Tempeff Inc. [27], and the deviations in corrugation depths in individual plates are less than 0.5%. Detailed

geometrical specifications of plates and exchangers are provided in Table 2. The authors could not reveal exact corrugation angles since it is patented information owned by the manufacturer [27]. Therefore, corrugation angles are specified with reference to the standard corrugation angle (β°), i.e., exchangers can be arranged in increasing order of corrugation angles as EXs 4, 1, and 5.

Table 2. Geometrical properties of corrugated exchangers

	Corrugation angle ($\beta°$)	h_{ch}/P_{ch}	L/h_{ch}	Number of flow channels (n_f)	Channel hydraulic diameter (m)
EX 1	β	0.13	49	14	0.0082
EX 2	β	0.13	116	14	0.0082
EX 3	β	0.13	232	14	0.0082
EX 4	$(\beta -29)$	0.13	50	14	0.0082
EX 5	$(\beta+21)$	0.13	52	14	0.0082
EX 6	β	0.25	73	9	0.0130
EX 7	β	0.36	59	7	0.0167

Corrugation depth
Corrugation angle
Length

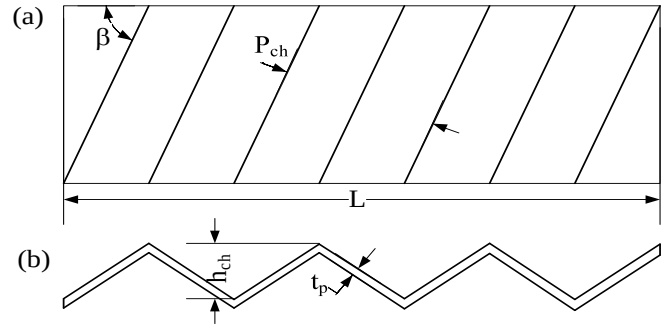

Fig. 3 Geometry of corrugated plates (a) top view (b) side view

The corrugated plate geometry is defined by pitch (P_{ch}): distance between two adjacent peaks or valleys measured perpendicular to the direction of corrugation, depth of corrugation (h_{ch}) and the thickness of plates (t_p). It should also be noted that the length and width of the plates are reported using their dimensions measured before providing corrugations.

The hydraulic diameter (D_h) of corrugated flow channels is defined in such a way that assuming it as parallel flow channels having channel width and height are equal to the

noncorrugated plate width and corrugation depth. The Reynolds number (Re) is determined using the channel velocity (V_{ch}) and hydraulic diameter and is given in Eqn. 1.

$$Re = \frac{\rho V_{ch} D_h}{\mu} \tag{1}$$

Where ρ and μ are the density and dynamic viscosity of the air, respectively.

Pressure drop and heat transfer coefficients are the important thermo-hydraulic performance parameters in the flow passages. The pressure drop is reported using the non-dimensional friction factor correlation [28], as presented in Eqn. 2.

$$f = \frac{|\Delta P| D_h}{\rho L V_{ch}^2/2} \tag{2}$$

To determine the heat transfer coefficient, the exchangers are exposed to the hot and cold airstreams (36°C and 24°C) alternatively, and the sensible effectiveness during hot and cold exposure periods (ε_{hot} and ε_{cold}) is calculated using Eqs. (3) and (4), respectively.

$$\varepsilon_{hot} = \frac{C_1}{C_{min}} \frac{(T_1 - \bar{T}_2)}{(T_1 - T_3)} \tag{3}$$

$$\varepsilon_{cold} = \frac{C_2}{C_{min}} \frac{(\bar{T}_4 - T_3)}{(T_1 - T_3)} \tag{4}$$

where T_1 and T_3 are the temperatures of the hot and cold inlet airstreams, and $\bar{T}_2$ and $\bar{T}_4$ are the time-averaged air temperatures at the exchanger outlets, respectively. C_1 and C_2 are the heat capacity rates of hot and cold airstreams, respectively and C_{min} is the minimum of C_1 and C_2. Then the overall number of transfer units (NTU_o) is determined using the experimental effectiveness with Kays and London correlation [29]. Subsequently, the heat transfer coefficient and Nusselt number are calculated using Eqs. (5) and (6).

$$\mathrm{NTU_o} = \frac{1}{\min((C)_1, (\mathrm{C})_2)} \left[\frac{1}{1/(\mathrm{hA_{ht}})_1 + 1/(\mathrm{hA_{ht}})_2} \right] \tag{5}$$

$$Nu = \frac{hD_h}{k_f} \tag{6}$$

Where h and k_f are the heat transfer coefficient and thermal conductivity of air. The detailed method of evaluating heat transfer coefficients and their uncertainty is reported in our previous publication [30].

2.3 Uncertainty analysis

The overall uncertainty in measurements is estimated from random (P_x) and bias (B_x) uncertainties for 95% confidence interval according to ASME PTC standard 19.1 [31] as given in Eqn. (7):

$$U = \sqrt{P_x^2 + B_x^2} \tag{7}$$

Random uncertainty is determined using Eqn. (8)

$$P_x = \frac{t\,SD}{N} \tag{8}$$

Where t and SD are student t-factor for 95% confidence interval for a degree of freedom of (N-1) and standard deviation. Bias uncertainty includes the calibration and data reduction errors. More details on instrumentation and uncertainty analysis are reported previously [24].

The experimental uncertainties in Reynolds number, friction factor, and Nusselt number were calculated from the uncertainties in flow rate, pressure drop, and temperature measurements according to the uncertainty propagation equation (Eqn. 9) and are included with respective results.

$$U_R = \left[\sum_{i=1}^{j}\left(\frac{\partial R}{\partial p_i}\,U_{p_i}\right)^2\right]^{0.5} \tag{9}$$

where U_R, U_{pi}, and $\partial R/\partial p_i$ are the total uncertainty, uncertainty in individual measurement Pi and the sensitivity coefficient of measurement Pi, respectively.

3. RESULTS AND DISCUSSIONS

In this section, the effects of the corrugation angle, the ratio of corrugation depth to pitch, length of the plate on average Nusselt number, and friction factor are reported. Different sets of correlations are developed for the average Nusselt number and friction factor based on the test data. It should be noted that the average Nusselt number is written as Nusselt number from here onwards.

3.1 Effect of corrugation angle

The effect of corrugation angle on the friction factor and Nusselt number are investigated using EXs 1, 4, and 5, and the results are compared in Fig. 4. As depicted in Table 2, these exchangers have similar geometry but different corrugation angles. Among these three exchangers,

EXs 4 and 5 have the least and highest corrugation angles. Similar to parallel plate EXs (where the flow is assumed to be laminar), the friction factor of corrugated EXs decreases with an increase in Reynolds number for the tested conditions, as shown in Fig. 4(a). From Fig. 4(a) and (b), the Nusselt number and friction factor are highest for EX 1($\beta°$) compared to EX 4 (β–29°) and EX 5 (β+21°).

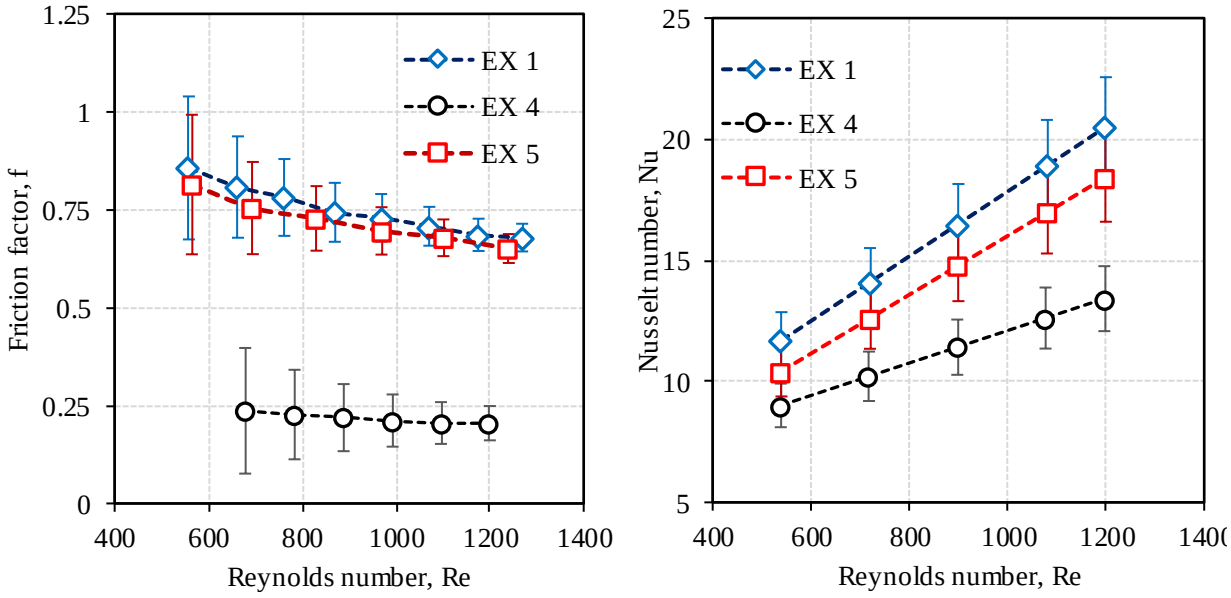

(a) (b)

Fig. 4 Effect of corrugation angle on (a) friction factor and (b) Nusselt number of triangular cross-corrugated exchangers

The complex three-dimensional flow through the cross corrugated channels strongly influences the heat transfer process. At low corrugation angles (EX 4: β–29°), the majority of flow follows the direction of corrugations and gets reflected at the sidewalls of the exchanger, and this type of flow is known as furrow flow, which is very similar to ordinary duct flow as reported by [11,13,19]. At a higher corrugation angle (EX 5: β+21°), most of the fluid follows a parallel zig-zag pattern in the longitudinal direction (along the exchanger length) and is called longitudinal wavy flow [19]. It should also be noted that the presence of more contact points between the adjacent plates at high corrugation angles causes flow separation and reduces the heat transfer [12]. The high heat transfer performance at intermediate corrugation angle (EX 1: $\beta°$), is due to the mixing of longitudinal and furrow flows (mixing flow), which induces secondary swirls in the flow along the direction of corrugations [10,19]. The findings of the present study are also in agreement with the literature conclusions, i.e., the highest Nusselt number is reported for EX 1,

which has the intermediate corrugation angle. Therefore, based on the above-tested h_{ch}/P_{ch}, ratio, the plates with intermediate corrugation angles have superior performance than plates with the highest and lowest corrugation angles. This also confirms the literature data, i.e., for sinusoidal corrugations, the optimum corrugation angles for maximum heat transfer are approximately 42°, 60°, and 70° for h_{ch}/P_{ch} of 0.14, 0.2 and, 0.27, respectively [10,12].

3.2 Effect of corrugation depth to pitch (h_{ch}/P_{ch}) ratio

The effect of h_{ch}/P_{ch} ratio on friction factor and Nusselt number are studied using EXs 1, 6, and 7 and shown in Fig. 5(a) and (b). Unlike parallel flow channels (where the flow is fully developed), the friction factor and Nusselt number of corrugated EXs increases with an increase in h_{ch}/P_{ch} ratio (or channel height). The highest and lowest Nusselt numbers are observed for EXs 7 and 1, respectively, which indicates that the heat transfer rate increases with an increase in corrugation depth (or h_{ch}/P_{ch} ratio). At higher corrugation depths (EX 7), the furrow component of the flow is significant, and as the corrugation angle increases, the longitudinal wavy flow becomes dominant [12]. Effective mixing of the furrow and longitudinal flow at higher corrugation depths and intermediate corrugation angles results in higher heat transfer rates [10,21]. Results from the present study are also in agreement with the findings of Dovic and Svaic [10,21], Zimmerer et al. [19], and Gasier and Kottke [12], i.e., an increase in corrugation depth at intermediate corrugation angles leads to high heat transfer.

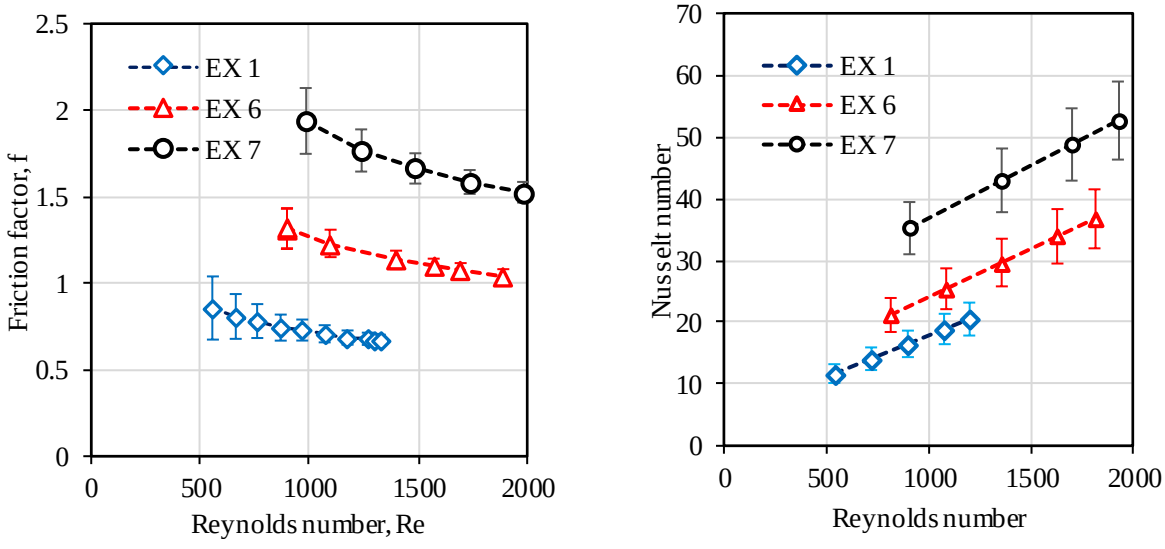

(a) (b)

Fig. 5 Effect of corrugation depth to pitch ratio on (a) friction factor and (b) Nusselt number of triangular cross-corrugated exchangers

3.3 Effect of plate length

All tested EXs have an aspect ratio of 0.05 (ratio of corrugation depth to channel width), and the tests were performed in exchangers with closed sidewalls. Unlike parallel plate EXs, the boundary layer separation and mixing of fluids due to complex flow patterns occur throughout the length of flow in corrugated EXs. The effect of the exchanger length (in the direction of airflow) on the heat transfer and friction factor has been studied using EXs 1, 2, and 3, and the results are presented in Fig. 6(a) and (b). It is found that the friction factor of EX 1 is lower than the other two exchangers, especially at lower Reynolds numbers. However, all the results are within the experimental uncertainties. Similarly, the maximum deviation in the Nusselt number for the three tested exchangers is less than 15%. Therefore, it is reasonable to conclude that the plate length has no significant effect on the friction factor and Nusselt number.

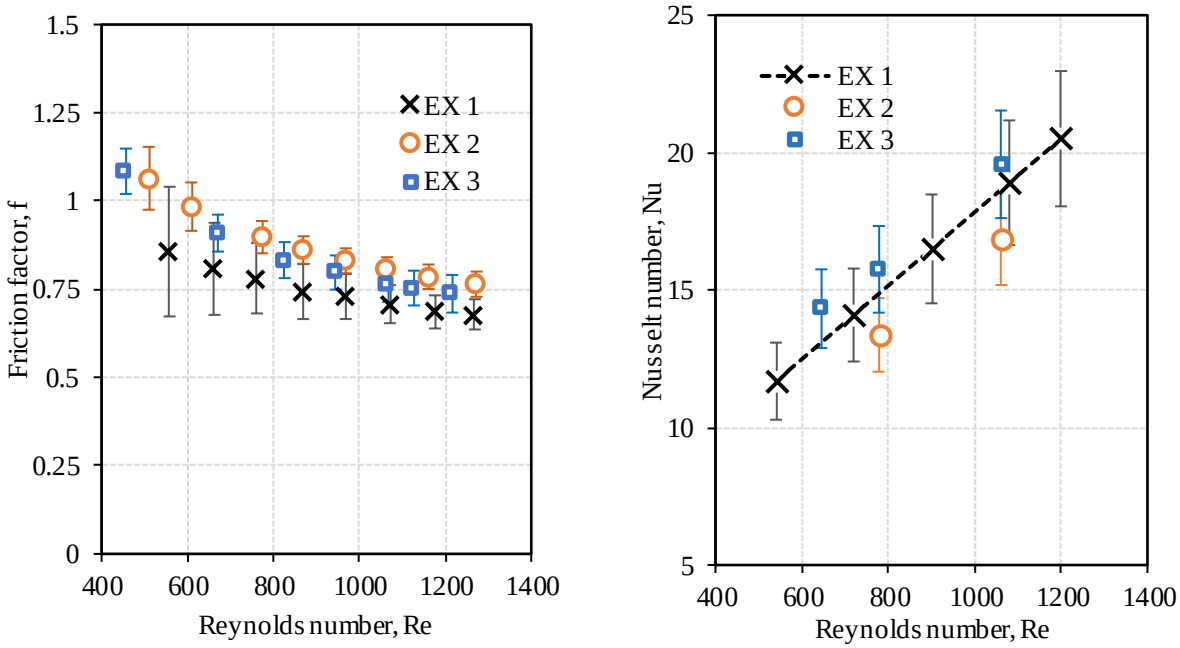

(a) (b)

Fig. 6 Effect of plate length on the (a) friction factor and (b) Nusselt number of triangular cross-corrugated exchangers

The hydraulic diameter measurements of flow channels are critical as it affects Reynolds number, Nusselt number, and friction factor estimations. The effect of uncertainty in hydraulic diameter measurements on these results is evaluated by an uncertainty analysis using Eqn. 9. The

analysis has been performed for the test conditions corresponding to the Reynolds number 640±13. Fig. 7 shows the change in relative uncertainty in Reynolds number, Nusselt number, and Friction factor for 0-4% deviations in hydraulic diameter. It can be inferred that a 4% deviation in hydraulic diameter measurements increases the relative uncertainty in Reynolds number, Nusselt number, and Friction factor by 2%, 0.6%, and 0.4%, respectively. It should also be noted that the contribution of uncertainty in pressured drop (across the exchanger), flow rate, and heat transfer coefficient measurements contribute predominantly to the overall uncertainty in friction factor, Nusselt number, and Reynolds number, respectively.

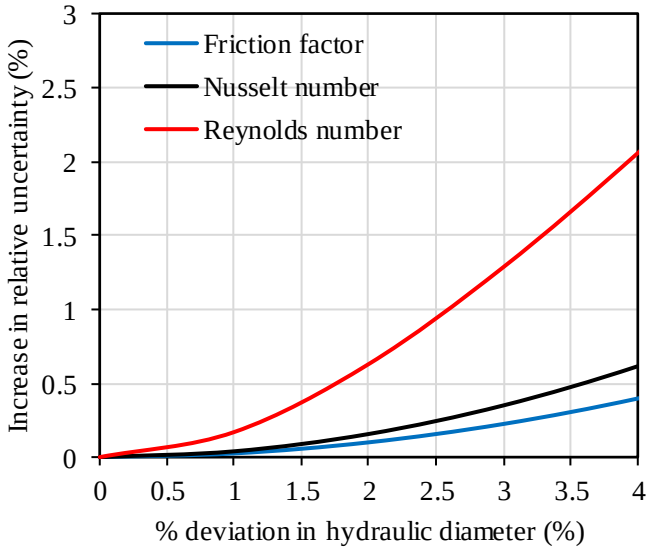

Fig. 7 Effect of % deviation in hydraulic diameter in overall uncertainty of friction factor, Nusselt number, and Reynolds number

3.4 Correlations for friction factor and Nusselt number

Empirical correlations for friction factor and Nusselt number are developed for the exchangers considered for studying the effect of corrugation angle and depth as functions of Re (Eqs. (10) and (11)) using least square curve fit methods. The fitting coefficients a, b, and coefficient of determination of fit (R^2) are reported in Table 3. The correlation results and experimental data agree with each other within ±5% for the friction factor and Nusselt number. The comparison between test data and predictions are also plotted in Fig. 8.

$$f_p = a_1 Re^{n_1} \tag{10}$$

$$Nu_p = a_2 Re^{n_2} Pr^{1/3} \tag{11}$$

Table 3. Correlation Coefficients of friction factor and Nusselt number (Eqs. (10) and (11))

EX	Friction factor			Nusselt number		
	a_1	n_1	R^2	a_2	n_2	R^2
EX 1	4.791	0.369	0.996	0.146	0.713	0.999
EX 4	2.901	0.369	1.000	0.217	0.698	0.997
EX 5	4.707	0.278	0.993	0.851	0.561	0.999
EX 6	11.598	0.320	0.999	0.410	0.507	0.999
EX 7	16.163	0.311	0.984	0.122	0.723	0.996

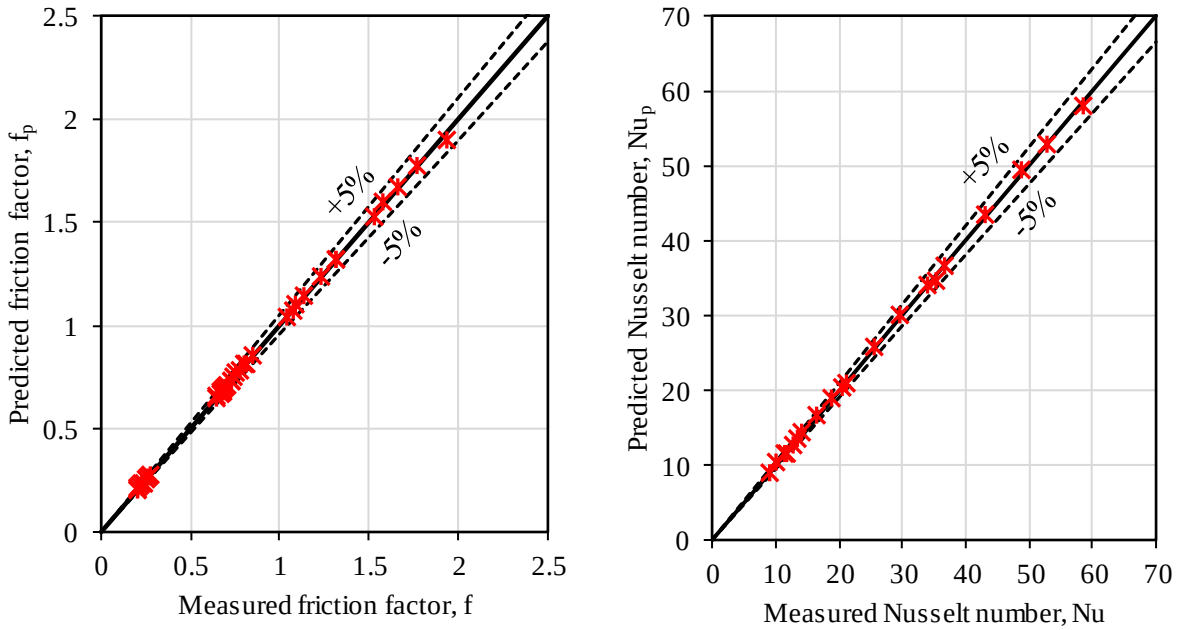

(a) (b)

Fig. 8 Comparison of experimental (a) friction factor and (b) Nusselt number with predictions (Eqs. (10) and (11))

From the experimental data, generalized correlations for friction factor and Nusselt number are developed as functions of corrugation angle, depth to pitch ratio, and Reynolds number, and are shown in Eqs. (12) and (13). The agreement between the predicted friction factor (Fig. 9(a)) and Nusselt number values (Fig. 9(b)) with the test data is within ±15%, respectively, for most of the operating conditions. The deviations between test data and measurements are highest at lower corrugation angles. However, higher Nusselt numbers are reported at high corrugation angles, and for high corrugation angles, the correlations show a good agreement with the test data (<±5%). It should be noted that both the correlations (Eqns. (12) and (13)) are developed using the test data for $0.13 < h_{ch}/P_{ch} < 0.36$ and $25° < \beta < 75°$.

$$f_p = 44.60\left[\left(\frac{\beta\left(h_{ch}/P_{ch}\right)^2}{Re}\right)^{9.32} + \frac{1}{\left(\frac{25056\, e^{(0.05\beta)}}{Re}\right)^{16.2}}\right]^{0.066} \quad (12)$$

$$Nu_p = 0.205\left(0.276Re^{3/4} f^{1/2}\right)^{5/4} Pr^{1/3} \quad (13)$$

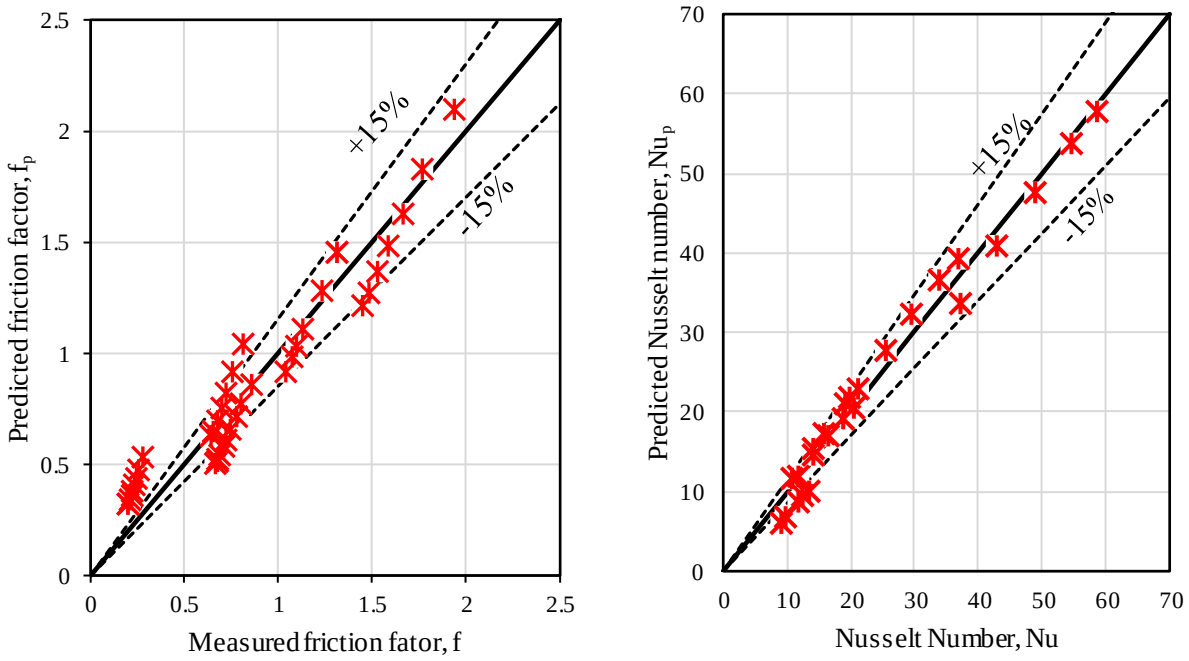

(a) (b)

Fig. 9 Comparison of experimental and predicted (a) friction factor and (b) Nusselt number

3.5 Comparison of test data with literature

The published literature related to heat transfer and pressure drop in cross-corrugated passages[1,9,11,12,22,32,33] is compared with the results of this study. Fig. 10 (a) shows the comparison of friction factor for corrugation angles ranging from 25°–80° for sinusoidal (by Gasier and Kottke [12]) and triangular configurations (test data from the present study). It should be noted that the data extracted from the literature are modified according to definition of the corrugation angle and h_{ch}/P_{ch} ratio presented in this paper. Also, the literature results (Fig. 10(a)) correspond to the Reynolds number 2000, whereas the results of this study are obtained at Reynolds number 1250. However, from Fig. 6, it is clear the friction factor is nearly constant at high Reynolds numbers. Therefore, the qualitative comparison of test data and literature is reasonable. It can be concluded that, like sinusoidal corrugations, the Nusselt number is highest at

intermediate corrugation angles compared to low and high corrugation angles. However, more number of experiments have to be conducted to determine the optimum corrugation angle for the maximum heat transfer.

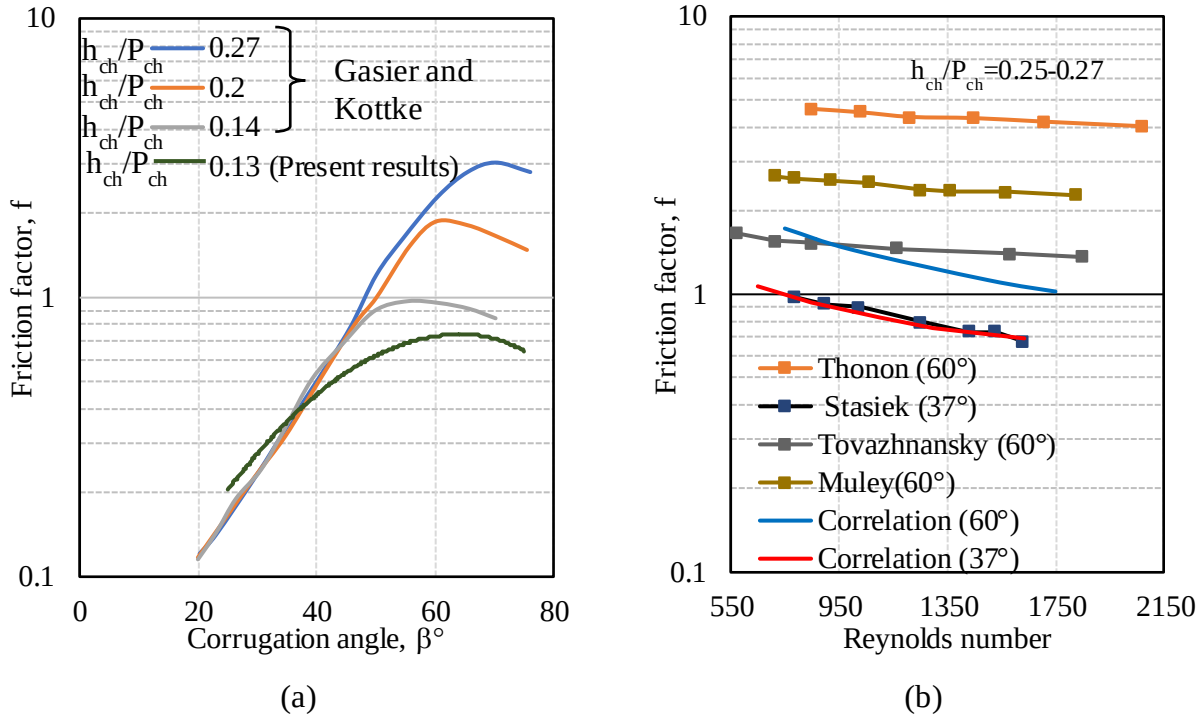

Fig. 10 Comparison of friction factor results with literature data

A comparison of the friction factor predicted from the correlation (Eqn. 12), and literature is presented in Fig. 10 (b). The plate configuration studied by Tovazhnyansky [22] is similar to this paper, and the correlation is in satisfactory agreement with his results compared to published data. Results of Muley [9] and Thonon [34] are based on sinusoidal configuration, and their results differs nearly by three times from each other . It is evident from the literature comparison that, similar to sinusoidal corrugation, increasing h_{ch}/P_{ch} increases the friction factor for intermediate corrugation angles. The higher friction factor values in literature data could be due to the difference in the corrugation pattern and experimental uncertainties.

The comparison of heat transfer performance is presented using $Nu/Pr^{0.4}$ with corrugation angle and Reynolds number (Nu is divided by $Pr^{0.4}$ to nullify the influence of Pr) in Fig. 11(a) and (b). From the literature comparison (Fig. 11 (a)), the Nusselt number increases with an increase in the corrugation angle initially. However, this trend is significant only at intermediate corrugation angles, which agrees with the findings presented in Fig. 4. The heat transfer results of Muley [9]

and Stasiek [1] are compared with the correlation and presented in Fig. 11(b), and the Nusselt number results from the literature are comparable with the prediction. The quantitative comparisons are not possible because, unlike triangular corrugations, there are no sharp edges in sinusoidal corrugations. The sharp edges of triangular corrugations favor additional mixing and improved heat transfer process, resulting in high Nusselt numbers. Besides, the heat transfer area enhancement ratio (ratio of the effective area due to corrugation to the projected area) is nearly 1.15-1.3 for the sinusoidal cross-corrugated plates reported in the literature whereas it is 1.1-1.15 in the present study.

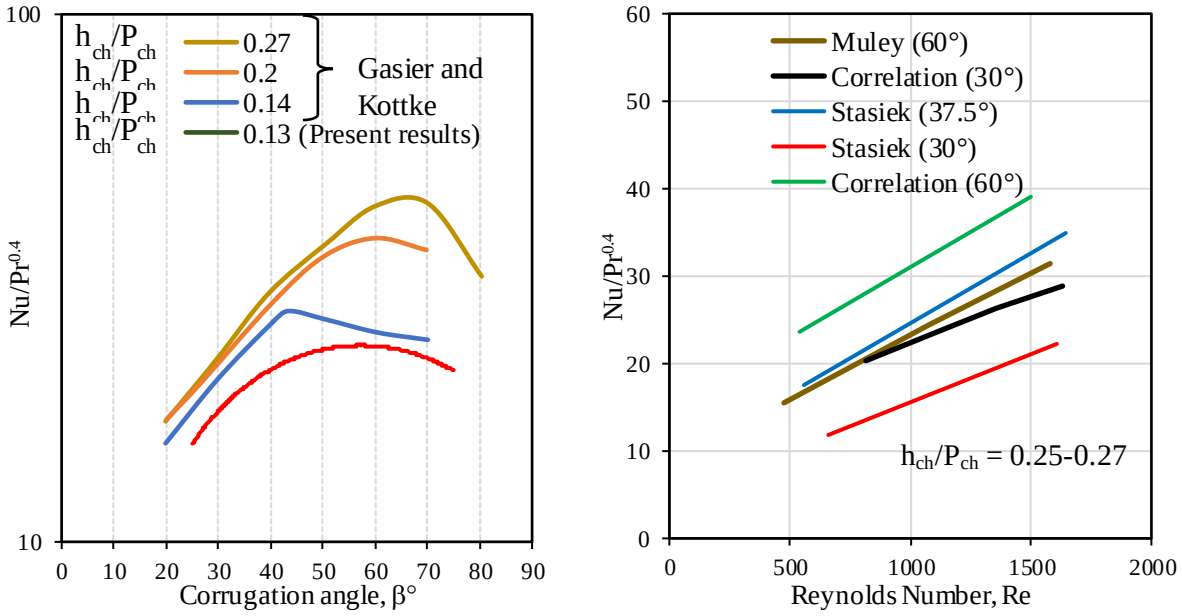

Fig. 11 Comparison of Nusselt number results with literature data

CONCLUSIONS

The thermo-hydraulic characteristics of triangular cross-corrugated flow passages are presented in this paper. The effects of corrugation angle, corrugation depth/pitch ratio, and plate length on average Nusselt number and friction factor are reported by testing representative compact heat exchangers. The average Nusselt number and friction factor (a) are highest for the exchanger having plates with intermediate corrugation angle (b) increases with an increase in the ratio of corrugation depth to pitch, and (c) is independent of the length of the plates on the direction of airflow. Finally, generalized correlations for the average Nusselt number and friction factor are developed based on the test data. The correlations and test data can be used as primary performance indicators for developing high-performance heat exchangers.

ACKNOWLEDGEMENTS

Financial support from the College of Engineering and Postdoctoral Studies of the University of Saskatchewan, National Science and Engineering Research Council (NSERC), Canada, Tempeff North America Inc., Winnipeg, Canada (Project No: 533225-18) are gratefully acknowledged. The support provided by Dr. Mohsen Shakouri (Canadian Light Source Inc.), Dr. Melanie Fauchoux, Mr. Hayden Reitenbach, and Mr. Shawn Reinink (Department of Mechanical Engineering, University of Saskatchewan) is also greatly appreciated.

REFERENCES

[1] J. Stasiek, M.W. Collins, M. Ciofalo, P.E. Chew, Investigation of flow and heat transfer in corrugated passages - I. Experimental results, Int. J. Heat Mass Transf. 39 (1996) 149–164. doi:10.1016/S0017-9310(96)85013-7.

[2] I. Gherasim, M. Taws, N. Galanis, C.T. Nguyen, Heat transfer and fluid flow in a plate heat exchanger part I. Experimental investigation, Int. J. Therm. Sci. 50 (2011) 1492–1498. doi:10.1016/j.ijthermalsci.2011.03.018.

[3] H. Ramin, E. Krishnan, C.J. Simonson, Fixed Bed Regenerators for HVAC Applications, in: Proc. 27th CANCAM, Sherbrooke, 2019: pp. 1–6. doi:10.3390/proceedings2019023004.

[4] H. Ramin, E.N. Krishnan, A. Gurubalan, W.O. Alabi, C.J. Simonson, Transient sensor errors and their impact on fixed-bed regenerator (FBR) testing standards, Sci. Technol. Built Environ. (2020) 1–22. doi:10.1080/23744731.2020.1846428.

[5] M. Faizal, M.R. Ahmed, Experimental studies on a corrugated plate heat exchanger for small temperature difference applications, Exp. Therm. Fluid Sci. 36 (2012) 242–248. doi:10.1016/j.expthermflusci.2011.09.019.

[6] T.S. Khan, M.S. Khan, M.C. Chyu, Z.H. Ayub, Experimental investigation of single phase convective heat transfer coefficient in a corrugated plate heat exchanger for multiple plate configurations, Appl. Therm. Eng. 30 (2010) 1058–1065. doi:10.1016/j.applthermaleng.2010.01.021.

[7] H.B. Luan, J.P. Kuang, Z. Cao, Z. Wu, W.Q. Tao, B. Sundén, CFD analysis of two types of welded plate heat exchangers, Numer. Heat Transf. Part A Appl. 71 (2017) 250–269.

doi:10.1080/10407782.2016.1264761.

[8] E.N. Krishnan, H. Ramin, G. Annadurai, C.J. Simonson, Influence of Plate Geometry on Sensible Effectiveness of Fixed-Bed Regenerators, Proc. 7th Int. Conf. Fluid Flow, Heat Mass Transf. (2020) 1–7. doi:10.11159/ffhmt20.185.

[9] A. Muley, R.M. Manglik, Experimental Study of Turbulent Flow Heat Transfer and Pressure Drop in a Plate Heat Exchanger With Chevron Plates, J. Heat Transfer. 121 (1999) 110–117. doi:10.1115/1.2825923.

[10] Dovic, Svaic, Influence of chevron plates geometry on performances of plate heat exchangers, Teh. Vjesn. 14 (2007) 37–45.

[11] W.W. Focke, J. Zachariades, I. Olivier, The effect of the corrugation inclination angle on the thermohydraulic performance of plate heat exchangers, Int. J. Heat Mass Transf. 28 (1985) 1469–1479. doi:https://doi.org/10.1016/0017-9310(85)90249-2.

[12] G. Gasier, V. Kottke, Effects of wavelength and inclination angle on the homogeneity of local heat transfer coefficients in plate heat exchangers, in: J.S. Lee (Ed.), Proc. 11th Int. Heat Transf. Conf., Kyongju, 1998: pp. 203–208.

[13] K. Sarraf, S. Launay, L. Tadrist, Complex 3D-flow analysis and corrugation angle effect in plate heat exchangers, Int. J. Therm. Sci. 94 (2015) 126–138. doi:10.1016/j.ijthermalsci.2015.03.002.

[14] V.S. Gullapalli, B. Sundén, CFD simulation of heat transfer and pressure drop in compact brazed plate heat exchangers, Heat Transf. Eng. 35 (2014) 358–366. doi:10.1080/01457632.2013.828557.

[15] S. Harikrishnan, S. Tiwari, Effect of skewness on flow and heat transfer characteristics of a wavy channel, Int. J. Heat Mass Transf. 120 (2018) 956–969. doi:10.1016/j.ijheatmasstransfer.2017.12.120.

[16] X. Zhu, F. Haglind, Relationship between inclination angle and friction factor of chevron-type plate heat exchangers, Int. J. Heat Mass Transf. 162 (2020) 120370. doi:10.1016/j.ijheatmasstransfer.2020.120370.

[17] X. Zhu, J.H. Walther, D. Zhao, F. Haglind, Transition to chaos in a cross-corrugated

channel at low Reynolds numbers, Phys. Fluids. 31 (2019). doi:10.1063/1.5122305.

[18] J.E. Hesselgreaves, R. Law, D.A. Reay, Chapter 6 - Surface Types and Correlations, in: J.E. Hesselgreaves, R. Law, D.A.B.T.-C.H.E. (Second E. Reay (Eds.), Compact Heat Exch. (Second Ed., Butterworth-Heinemann, 2017: pp. 221–274. doi:https://doi.org/10.1016/B978-0-08-100305-3.00006-9.

[19] C. Zimmerer, P. Gschwind, G. Gaiser, V. Kottke, Comparison of heat and mass transfer in different heat exchanger geometries with corrugated walls, Exp. Therm. Fluid Sci. 26 (2002) 269–273. doi:10.1016/S0894-1777(02)00136-X.

[20] E.M. Sparrow, L.M. Hossfeld, Effect of rounding of protruding edges on heat transfer and pressure drop in a duct, Int. J. Heat Mass Transf. 27 (1984) 1715–1723. doi:10.1016/0017-9310(84)90154-6.

[21] D. Dović, B. Palm, S. Švaić, Generalized correlations for predicting heat transfer and pressure drop in plate heat exchanger channels of arbitrary geometry, Int. J. Heat Mass Transf. 52 (2009) 4553–4563. doi:10.1016/j.ijheatmasstransfer.2009.03.074.

[22] L. Tovazhnyansky, P. Kapustenko, V.. Tsibulnic, Heat transfer and hydraulic resistance in channels of plate heat exchangers, Energetika. 9 (1980) 123–125.

[23] O.P.. Arsenyeva, L. Tovazhnyansky, P. Kapustenko, G. Khavin, The generalized correltaion for friction factor in criss cross flow channels of plate heat exchangers, Chem. Eng. Trans. 25 (2011) 399–404.

[24] E.N. Krishnan, H. Ramin, M. Shakouri, L.D. Wilson, C.J. Simonson, Development of a small-scale test facility for effectiveness evaluation of fixed-bed regenerators, Appl. Therm. Eng. 174 (2020). doi:10.1016/j.applthermaleng.2020.115263.

[25] E.N. Krishnan, H. Ramin, C.J. Simonson, Performance Testing of Fixed-Bed Regenerators for HVAC Applications, in: Proc. 2nd Pacific Rim Therm. Eng. Conf., Hawaii, United States, 2019: pp. 1–5.

[26] ISO, International Standard: ISO 5167-1 Measurement of fluid flow by means of pressure differential devices inserted in circular cross-section conduits running full--Part 1: General principles and requirements, Geneva, 2003.

[27] Tempeff North America, The Dual Core Difference, (n.d.). https://www.tempeffnorthamerica.com/dual-core-heat-recovery/ (accessed May 17, 2020).

[28] Shah R.K, London A.L, Advances in Heat Transfer, Laminar Flow Forced Convection in Ducts, Academic Press, New York, 1978.

[29] R.K. Shah, D.P. Sekulic, Fundamentals of heat exchanger design, New Jersey, 2004. doi:10.1007/bf00740254.

[30] E.N. Krishnan, H. Ramin, A. Gurubalan, W.O. Alabi, C.J. Simonson, Methodologies for predicting the effectiveness of fixed-bed regenerators from small-scale test data, ASME J. Therm. Sci. Eng. Appl. submitted (2020).

[31] ASME/ANSI, Performance Test Code 19.1 Test Uncertainty: Instruments and Apparatus, New York, 1998.

[32] M. Ciofalo, J. Stasiek, M.W. Collins, Investigation corrugated of flow and heat transfer Numerical simulations, Int. J. Heat Mass Transf. 39 (1996) 165–192.

[33] O.P. Arsenyeva, L.L. Tovazhnyanskyy, P.O. Kapustenko, O. V. Demirskiy, Heat transfer and friction factor in criss-cross flow channels of plate-and-frame heat exchangers, Theor. Found. Chem. Eng. 46 (2012) 634–641. doi:10.1134/S0040579512060024.

[34] B. Thonon, R. Vidil, C. Marvillet, Recent research and developments in plate heat exchangers, J. Enhanc. Heat Transf. 2 (1995) 149–155. doi:10.1615/JEnhHeatTransf.v2.i1-2.160.